SANDIA REPORT

SAND94—0603 • UC—704

Unlimited Release

Printed April 1994

A Capillary Flow Test for Printed Wiring Boards

F. G. Yost, F. M. Hosking, D. R. Frear, D. O. MacCallum

Prepared by
Sandia National Laboratories
Albuquerque, New Mexico 87185 and Livermore, California 94550
for the United States Department of Energy
under Contract DE-AC04-94AL85000

24p.

Issued by Sandia National Laboratories, operated for the United States Department of Energy by Sandia Corporation.

SAND94-0603
Unlimited Release
Printed April 1994

Distribution
Category UC-704

A CAPILLARY FLOW TEST FOR PRINTED WIRING BOARDS

F. G. Yost, F. M. Hosking, D. R. Frear, and D. O. MacCallum
Center for Solder Science and Technology
Sandia National Laboratories
Albuquerque, NM 87185-5800

A CAPILLARY FLOW TEST FOR PRINTED WIRING BOARDS

F. G. Yost, F. M. Hosking, D. R. Frear, and D. O. MacCallum
Center for Solder Science and Technology
Sandia National Laboratories
Albuquerque, NM 87185-5800

ABSTRACT

A test vehicle was designed and fabricated with the use of printed wiring board materials and standard manufacturing processes. Solder was placed on a circular metallization pattern and when melted, wets onto a connected strip of metallization. Capillary equilibrium conditions were determined and used to demonstrate that flow onto the strip will be prevented for critical circle and strip dimensions. A model for the rate of flow onto the strip was derived and compared to experimental results. Reasonable fits to the data were made and a kinetic coefficient so obtained was compared to calculated values based upon available surface energy and liquid viscosity data. The analysis leads to the conclusion that the standard Poiseuille approach to capillary flow is adequate for describing these kinetics.

INTRODUCTION

The modern understanding of capillary flow began with the work of Poiseuille[1] who experimentally characterized the steady flow of liquid from one vessel to another through a slender tube. He found that the volume flow rate was proportional to the hydrostatic pressure head between the two vessels and inversely proportional to the length of the tube. In 1906 Bell and Cameron[2] were studying flow of water through soil and modelled this process as flow through capillary tubes. They transformed Poiseuille's description of flow into a differential equation which predicted parabolic capillary penetation behavior given by:

$$x^2 = Kt$$

where x is the capillary penetration distance, t is time, and K is a constant. This simple model exhibited very good agreement with their data. Washburn[3] was the first to lend a theoretical interpretation to this behavior. With the results of Poiseuille, Washburn showed that the rate of penetration due to capillary pressure alone is:

$$\frac{dx}{dt} = \frac{\gamma r Cos\Theta_o}{4\eta x}$$

where γ is surface tension of the liquid, r is the radius of the capillary, η is the liquid viscosity, and Θ_o is the equilibrium contact angle between liquid and capillary. Washburn appreciated the time dependence of Θ_o, but his measurements were not accurate enough to resolve it. This expression predicts parabolic behavior and provides interpretation for the constant K. Latin[4] was the first to use the integrated form of Washburn's equation on the capillary flow of solder between copper plates. Notwithstanding the many attempts to improve this model through the ensuing years, parabolic behavior continued to lie at the root of all treatments[5-7]. Semlak and Rhines[8] found excellent agreement with the Washburn equation for the penetration of various powdered metal compacts by liquid metals. They also provided a sensible interpretation of the capillary radius in porous materials. They concluded that the penetration process was controlled by liquid viscosity because of the agreement between their experimentally derived activation energies and available data for temperature dependence of viscosity. Engineering studies of solder flow into gaps between parallel plates have also been studied by Humpston and Jacobson[9] and by Wolverton and Ables[10]. Process recommendations for joint filling and hermetic sealing were provided.

The purpose of the work described in this report is to evaluate and model the behavior of a test vehicle that captures certain aspects of capillary behavior. The test vehicle (TV) is a small printed wiring board (approximately 4 x 5 cm^2) that has been photolithographically prepared by standard processes. The metal pattern is designed so that the vehicle can be mounted at a controlled spacing from another test board with the facing patterns being a mirror image of each other. Solder wetting of the metallization then occurs in the capillary gap between the two specimens. However, it was decided to investigate solder wetting behavior on a single test vehicle before testing of the matched capillary configuration. In the work reported below, the geometry of the test vehicle is defined, the conditions for wetting are described, the kinetics of wetting are modelled after the work cited above, and wetting test results are discussed in light of the model analysis.

CONDITIONS FOR WETTING

Consider a circular metallization pattern having radius, r_c, and let a small volume of solder wet and spread to a radius $r < r_c$ such that capillary equilibrium is obtained at a contact angle, Θ_o. Let the solder volume be increased to a value V_o just large enough to allow the solder to spread to the metallization radius. Any further increase of volume will increase the contact angle to a value $\Theta_+ > \Theta_o$, but will not increase the radius since

wettable metallization extends only as far as r_c. In this quadrajunction configuration, there exists an excess pressure which would drive flow of solder should more metallization be made available. Consider additional metallization in the form of a very slender rectangular strip of width $\delta < r_c$ connected to the circular piece as illustrated in Figure 1. The excess pressure will tend to move solder onto the strip for certain values of the ratio δ to r_c. Solder will then flow a distance, x, reducing the pressure over the circular metallization until it equals that above the strip. To simplify the calculation of these conditions, it will be assumed that the configuration geometry is small enough to neglect the effect of gravity on solder shape. Thus, the solder on the circular metallization has a spherical cross section while the solder on the strip is circular. The height of solder on the strip is given by:

$$h_s = \frac{\delta}{2}\left(\frac{1-\cos\Theta_s}{\sin\Theta_s}\right)$$

where Θ_s is the equilibrium contact angle on the strip. The mean curvature of the solder surface on the strip is:

$$\frac{1}{R_s} = \frac{2\sin\Theta_s}{\delta}$$

and the capillary pressure is

$$P_s = \frac{2\gamma\sin\Theta_s}{\delta} \qquad [1]$$

After solder flows onto the strip, a contact angle, Θ_c, is established on the circular metallization and the capillary pressure is given by:

$$P_c = \frac{2\gamma\sin\Theta_c}{r_c}\,. \qquad [2]$$

In mechanical equilibrium, the capillary pressures, given by eqs. 1 and 2, must be equal which yields the geometric condition for wetting:

$$\frac{\delta}{r_c} = \frac{\sin\Theta_s}{\sin\Theta_c} \qquad [3]$$

If the strip length is sufficiently long, excess pressure will be zero and since $\delta \neq r_c$, equilibrium, according to eq. 3, must involve contact angle hysterisis if the strip and circular metallizations are identical. Contact angle is known to be a function of the wetting velocity and even exhibits a range or band of static values, $2\Delta\Theta$, in mechanical equilibrium. These phenomena are collectively called contact angle hysterisis[11-13]. Contact angle hysterisis is usually attributed to substrate surface roughness and chemical heterogeneity, common to most real surfaces, and can slow the smooth advance of the wetting front. With eutectic Sn-Pb solder on rolled copper sheet (with mildly activated rosin flux), observed capillary angles range from approximately 10° to 20°. If Θ_o is

defined as the Young contact angle, it will lie at the approximate center of the range of contact angle hysterisis. For an equilibrium capillary configuration, Θ_s and Θ_c must be within or define the extremities of the range of stable contact angles, $2\Delta\Theta$. As solder flows onto the strip, it is reasonable to propose that Θ_+ decreases to a contact angle $\Theta_c = \Theta_o + \Delta\Theta$. For a given geometry, eq. 3 then specifies what value Θ_s must take for equilibrium. Figure 2 shows the relationship of Θ_s and Θ_c for various choices of δ / r_c. For a Young angle of 15° and a hysterisis range of $2\Delta\Theta$=10°, it is clear that for this range of contact angles, δ / r_c must be greater than approximately 0.5 if flow is to occur onto the strip. Only in this way will the two contact angles be contained by the stable hysterisis band. Note that if δ / r_c=0.25, there exists no combination of Θ_s and Θ_c lying within the $2\Delta\Theta$ hysterisis band that satisfy eq. 3. This implies that flow will not occur onto a strip having this ratio.

ANALYSIS OF KINETICS

The pressure drop along the strip is taken to be $\Delta P = P_c - P_s$ and the kinetics of Poiseuille flow are:

$$\frac{dx}{dt} = \frac{A_s B}{x}\left(\frac{\sin\Theta}{r_c} - \frac{\sin\Theta_s}{\delta}\right) \qquad [4]$$

where, x is the distance solder has flowed onto the strip, t is time measured from the commencement of flow onto the strip, θ is the temporal contact angle on the circle, and A_s is the cross sectional area of solder on the strip given by:

$$A_s = \frac{1}{8}\left(\frac{\delta}{\sin\Theta_s}\right)^2 (2\Theta_s - \sin 2\Theta_s) \qquad [5]$$

and

$$B = \frac{\gamma}{16\pi\eta}.$$

Four (each) measurements of the contact angle on the strip of three solder-tested TVs to characterize their contact angles, Θ_s. The overall average contact angle was 15.6 degrees while the standard deviation was 4.4 degrees. The average contact angle, during flow, was constant relative to that on the circular metallization which decreased in time as flow commenced down the strip. The solder volume, V_o, is given by:

$$V_o = \frac{\pi}{6} h(x)\left(3r_c^2 + h^2(x)\right) + A_s x \qquad [6]$$

where $h(x)$ is the height of the solder on the circle given by:

$$h(x) = r_c\left(\frac{1-\cos\Theta}{\sin\Theta}\right) \qquad [7]$$

The solder mass (10.1 mg) was kept constant during the experiments and was converted to volume with use of the density (7.91 g/cm^3) given by Poirier[14]. As a result of reaction with the TV metallization, the volume of solder changes slightly during flow. A simple calculation shows that this volume change is very small so it was assumed that the volume of solder remained constant and equal to its initial value. For any x, eqs. 6 and 7 can be solved for Θ and substituted into eq. 4 and the resulting differential equation can be solved for x versus flow time. The parameters used for these solutions are shown in Table 1. The appropriate root to the volume constraint (eq. 6) was numerically calculated and used in the simultaneous solution of the non-linear system of eqs. 4-7. Solutions to these equations are shown in Fig. 3. To obtain these solutions several B values were chosen arbitrarily. Depending on the chosen B values, the solutions have parabolic character for the smaller B's while for larger B's they exhibit rapid wetting rates and a pronounced knee.

EXPERIMENTAL PROCEDURE

The TV, shown in Fig. 4, was fabricated using conventional printed wiring board (PWB) materials and fabrication technologies. The TV substrate, 0.152 cm thick, is an epoxy resin laminate reinforced with glass fiber cloth and the copper patterns were printed and etched according to standard procedure. Additional copper was electrodeposited to a final conductor thickness of 35 μm. Powder-free finger cots or latex gloves were worn when handling test specimens to minimize contamination from oils, greases, salts, or other foreign debris. Transporting of TVs was done with stainless steel tweezers by gripping along the TV edge. The TV design has duplicate test patterns with line width-to-pad radius ratios (δ / r_c) of 0.25, 0.5, 0.75, and 1.0. The pad radius is 0.102 cm, with line widths ranging from 0.025 to 0.101 cm. The line length (or maximum possible capillary flow) is 3.81 cm. One millimeter reference marks are also patterened onto the TVs and can be used as calibration or datum points during video image analysis of the specimens. A buss bar and connecting conductive lines between test patterns (not shown in Fig. 4) are incorporated into the TV design for electrodeposition of other metal surface finishes Soldermask and organic solderability preservative can also be applied to the TV.

Samples were cleaned before testing by degreasing in trichloroethylene and rinsing in isopropyl alcohol. They were then cleaned in a 10% HCl and deionized water solution for 3 minutes, rinsed in hot tap water, rinsed in deionized water, rinsed in isopropyl alcohol, and finally blown dry with technical grade nitrogen gas. This cleaning method

provides a consistent surface finish for testing. Test specimens were coated with flux following the precleaning step. A commercially available, mildly activated rosin-based flux was diluted with an equal volume of isopropanol and used for this flux coating. TVs were gently agitated in the flux bath for 5 to 10 seconds. After slow withdrawal from the flux, the TVs were held vertically for approximately 15 seconds and blotted along their bottom edges to remove excess flux. After fluxing and draining, solder pellets were placed on each TV pad. Solder pellets weighing 10.1 ± 0.1 mg were dipped in flux and placed immediately on the fluxed TV pads. A flux predry (or hold period) of 15-30 minutes before testing was used to volatilize the flux carrier and reduce test variability.

Tests were performed by floating the TVs on a standard thermostatically controlled pot containing eutectic Sn-Pb solder. The solder bath was sufficiently large to avoid touching the TV against the sides of the solder pot. Test temperatures were maintained within $\pm$ 2°C. The nominal baseline test temperature was 245°C. TVs were floated for 90-120 seconds, depending on the completion of capillary flow. Samples were carefully removed from the solder bath after testing to minimize agitation of the molten solder on the TV. This was accomplished by holding the TV in a horizontal position until the solder solidified. Flux residues were then removed by rinsing with trichloroethylene.

Capillary flow data were analyzed from recorded video images. A black and white, charged-coupled device camera and professional video tape recorder with time code generator were used to record the wetting images. The camera was mounted such that its lens axis was perpendicular to the surface of the floated TV. A fiber optic light source was used to illuminate the test surface. The images of solder flow captured on video tape were digitally analyzed to derive the kinetic data. Data were taken from the point at which the molten solder began to flow onto the strip portion of the TV; this time being defined as t=0. The images were captured from the video tape and stored on a hard disk attached to a personal computer. Digital analysis was performed on the stored images using commercially available image analysis software. The data were taken in sequence every second after t=0. The distance traveled is measured from the pad/strip intersection to the farthest distance solder had travelled. The data was compiled into a spreadsheet and plotted.

RESULTS

The most consistent wetting results were found for the 0.076 cm wide strip and this is the data that was used for further analysis. The 0.102 cm width did not consistently wet the

full length of the strip. Strip widths less than 0.076 cm resulted in constriction of solder flow and negligible wetting onto the strip. A typical example of a test vehicle after completion of the wetting test is shown in Fig. 4. The 0.076 cm wide strip has wetted most of its full length, all other widths wet a shorter portion of their length. The strip having width 0.025 did not wet at all as expected from the constraint implied by eq. 3.

Curves of distance wetted as a function of time from four tests, for the 0.076 cm thick strip, are shown in Figs. 5a and 5b. Figure 5a shows similar flow results obtained from two different TVs. Fig. 5b shows variable flow results from the matching patterns of the other two TVs. The data was divided using the pad-strip orientation for graphing and modeling purposes, since there seemed to be some direction-sensitive effects. A reasonable B value fit was made to each data set and is superimposed on the respective data plot. Soon after the solder melts, wetting generally occurs rapidly, followed by a parabolic slowing of the molten solder front. A magnified view of one of the solder wetting fronts is shown in the scanning electron microscope image of Fig. 6. A narrow region at the three phase line is suggestive of a reaction between solder and strip metallization.

Two of the four tested substrates gave similar wetting results on the matching 0.076 cm strips (Fig 5a). The flow rate and final wetted distance were approximately 0.15 cm/s and 3 cm, respectively. The length wetted generally plateaued 30 s after the start of solder flow. On the other two TVs, however, capillary flow initiation and final wetting appeared to be affected by the orientation of the matching strips (Fig 5b). The strip extending from the pad on the right side of the TV usually yielded better flow results. Flow from the right side preceded the left side by 10-20 seconds. The average flow rate and wetted distance data for this second test group were as follows:

(a) right to left flow - 0.09 cm/s and 2.5 cm

(b) left to right flow - 0.06 cm/s and 2.1 cm

The delayed start of wetting from the left pad resulted in reduced capillary flow, probably due to extended exposure of the strip's surface to the elevated test temperature and ambient. The time to reach equilibrium was also significantly longer ($\geq$ 50 s).

DISCUSSION AND CONCLUSIONS

By balancing the capillary pressure of the solder surface on the circular metallization and that on the strip a representation of capillary equilibrium has been obtained. This equilibrium expression implies that solder will not flow onto strips with δ / r_c smaller

than a critical value that depends on the equilibrium contact angle and on the size of the hysterisis band. For an equilibrium contact angle of 15 degrees and a hysterisis band of 10 degrees it was anticipated that the smallest δ / r_c would not allow flow. Experiments proved this to be correct since the only flow observed on the strip was a very small precursor foot. The capillary constriction presented by subcritical δ / r_c effectively prevents bulk fluid flow but does not restrict mass transport that leads to the formation of the precursor. In effect, the capillary flow TV provides a convenient way to study the precursor phenomenon.

Flow kinetics were derived in the manner of Poiseuille by equating a viscous dissipation to the driving force for wetting. This yielded an equation for the rate of spreading that could be solved by assuming that the spreading solder droplet was spherical and that volume is conserved. The numerical solutions seemed to "fit" the data shown in Figs. 5a and 5b for B values of 80 and 40, respectively. Assuming a surface energy for liquid solder of 400 mJ/m^2 [15-17] and a bulk viscosity of 0.375 Pa s [18] gives a γ / η ratio of 10700 cm/s and a calculated B of 212 cm/s. It has been shown that capillary flow models based on Poiseuille kinetics significantly overestimate the rate of spreading of droplets on flat substrates [19-21]. One cause for this discrepancy is conjectured to be a difference between bulk fluid viscosity, as used above, and the effective viscosity at the three phase line where additional energy dissipation is caused by contact and flow against the substrate surface[22]. If the effective viscosity is just a factor of 4 larger than that for bulk very good agreement is obtained between the calculated B and the "fitted" value.

The left-to-right wetting differences were first thought to be caused by a temperature gradient that may have existed on the TV between the mirror imaged patterns. Thermocoupled experiments revealed no significant gradients over the top surface of a heated TV. A gradient (approx. 10-20°C) was measured between the top and bottom surfaces, but in all cases, each surface appeared to have a relatively uniform temperature. The wetting differences are probably related to the materials and processes used to fabricate the TV. To understand this wetting phenomenon will require further investigation. A TV redesign and more direct control of its fabrication are being considered to minimize possible test variability. To further reduce variability, the solder pellets could be spot welded to each specimen prior to fluxing and reflow. These changes are especially important if test consistency is to be improved.

ACKNOWLEDGEMENTS

The authors would like to extend their gratitude to Cindy Hernandez and Susan Sackinger of Sandia National Laboratories for their generous help during the course of this investigation. They would also like to thank the Surface Finishes Team of the National Center for Manufacturing Sciences Printed Wiring Board Project for their help and guidance. This work was performed at Sandia National Laboratories, which is supported by the U.S. Department of Energy under contract number DE-AC04-94AL85000.

REFERENCES

1. J. L. M. Poiseuille, *Ann. Chim. Phys.*, 1843, vol. 7, pp. 50-74.
2. J. M. Bell and F. K. Cameron, *J. Phys. Chem.*, 1906, vol. 10, pp. 658-674.
3. E. W. Washburn, *Phys. Rev.*, 1921, vol. 17, pp. 273-283.
4. A. Latin, *J. Inst. Metals*, 1946, vol. 72, pp. 265-282.
5. W. E. Brittin, *J. Appl. Phys.*, 1946, vol. 17, pp. 37-44.
6. R. M. Barrer, *Disc. Faraday Soc.*, 1948, No. 3, pp. 61-72.
7. J. R. Ligenza and R. B. Bernstein, *J. Am. Chem. Soc.*, 1951, vol. 73, pp. 4636-4638.
8. K. A. Semlak and F. N. Rhines, *Trans. AIME*, 1958, vol. 212, pp. 325-331.
9. G. Humpston and D. M. Jacobson, *GEC J. Research*, 1991, vol. 8, pp. 145-150.
10. M. Wolverton and B. Ables, *Soldering and Surface Mount Technology*, 1991, No. 9, pp.11-15.
11. R. Shuttleworth and G. L. J. Bailey, *Disc. Faraday Soc.*, 1948, No. 3, pp. 16-22.
12. N. K. Adam and G. Jessop, *J. Chem. Soc. London*, 1925, vol. 127, pp.1863-1868.
13. C. Hue and S. G. Mason, *J. Colloid and Interface Science*, 1977, vol. 60, pp. 11-38.
14. D. R. Poirier, *Met. Trans. A*, 1988, vol. 19A, pp. 2349-2354.
15. A. E. Schwaneke, W, L. Falke, and V. R. Miller, *J. Chem. and Eng. Data*, 1978, vol. 23, pp. 298-301.
16. D. W. G. White, *Met. Trans.*, 1971, vol. 2, pp. 3067-3071.
17. L. S. Goldman and B. Krall, *Rev. Sci. Instrum.*, 1976, vol. 47, pp. 324-325.
18. T. Ejima, Y. Sato, T. Yamamura, A. Hayashi, and T. Yamazaki, *J. Japan Inst. Metals*, 1990, vol. 54, pp.1005-1012.
19. J. C. Ambrose, M. G. Nicholas, and A. M. Stoneham, *Acta metall. mater.*, 1992, vol. 40, pp. 2483-2488 .
20. J. C. Ambrose, M. G. Nicholas, and A. M. Stoneham, *Acta metall. mater.*, 1993, vol. 41, pp. 2395-2401.

21. F. G. Yost, F. M. Hosking, and D. R. Frear, in*The Mechanics of Solder Alloy Wetting and Spreading*, F. G. Yost, F. M. Hosking, and D. R. Frear, eds., Van Nostrand Reinhold, New York, NY, 1993, pp. 1-7.
22. P. G. de Gennes, *Rev. Mod. Phys.* , 1985, vol. 57, pp. 827-863.

TABLE 1. A listing of parameters used for fitting wetting data to the model.

$\delta = 0.076$ cm

$r_c = 0.102$ cm

$\Theta_s = 15.6$ degrees

$\rho = 7.91$ g/cm^3

$m = 10.1$ mg

FIGURE CAPTIONS

Figure 1. Capillary flow test geometry for evaluating solder capillary flow. The ratio of line width to pad radius (δ/ρ) can be varied to control solder spreading from the metal base or pad onto the connected test strip.

Figure 2. Equilibrium contact angle of solder on circular metallization versus that on strip for various strip width to circle radius ratios.

Figure. 3 Calculations of the flow distance versus time for a strip having width 0.076 cm. Thekinetics parameter, B, was varied from 50 to 5000 and yielded a continuous family of shapes ranging from parabolic to step-like wetting.

Figure 4. The capillary flow test vehicle. Depending on the ratio δ/ρ solder flows onto the strip to a distance that provides capillary pressure equilibrium.

Figure 5a. Wetting results on test vehicles 1 and 2 distinguished according to number and flow direction. The average flow rate was 0.15 cm/s and a reasonable fit to the kinetics model gave B=80.

Figure 5b. Wetting results on test vehicles 3 and 4 distinguished according to number and flow direction. The average flow rate was 0.075 cm/s and a reasonable fit to the kinetics model gave B=40.

Figure 6. A scanning electron photomicrograph showing the wetting front. A reaction zone can be seen at the three phase line.

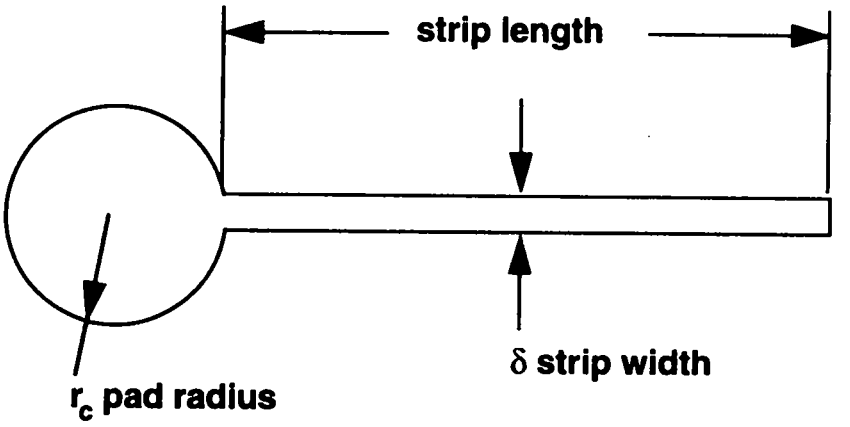

Figure 1. Capillary flow test geometry for evaluating solder capillary flow. The ratio of line width to pad radius (δ/ρ) can be varied to control solder spreading from the metal base or pad onto the connected test strip..

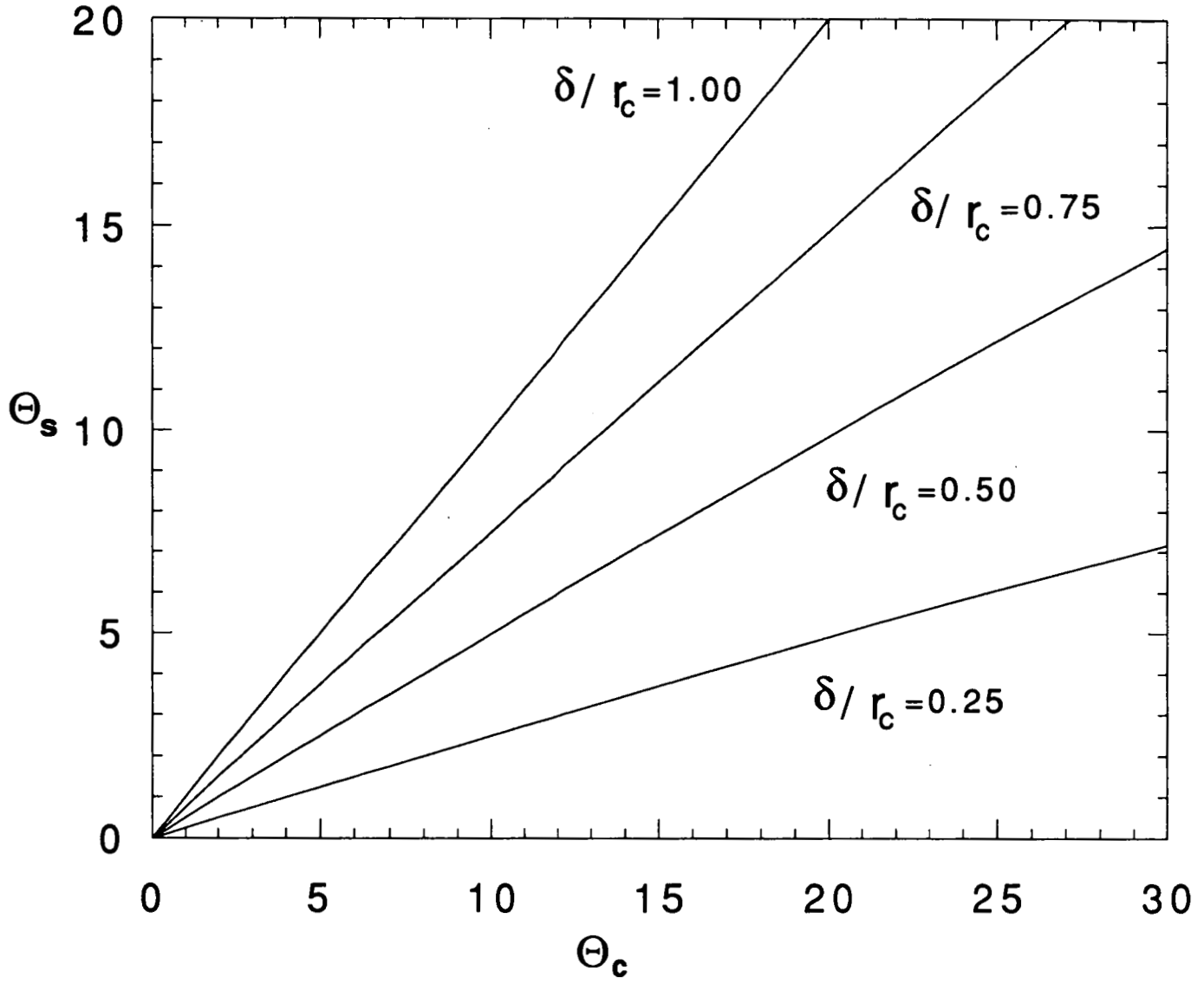

Fig. 2. Equilibrium contact angle of solder on circular metallization versus that on strip for various strip width to circle radii ratios.

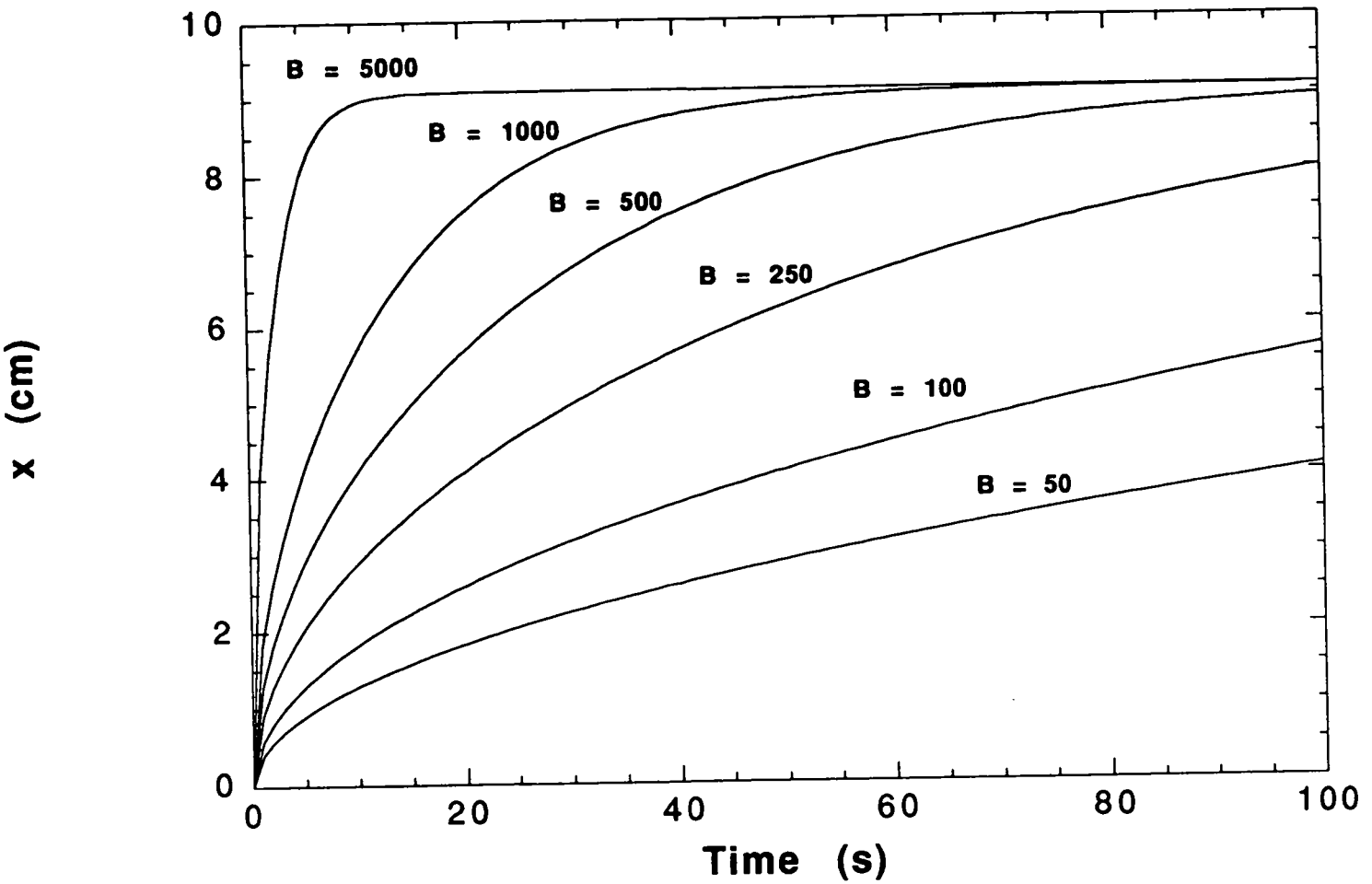

Figure. 3 Calculations of the flow distance versus time for a strip having width 0.076 cm. Thekinetics parameter, B, was varied from 50 to 5000 and yielded a continuous family of shapes ranging from parabolic to step-like wetting.

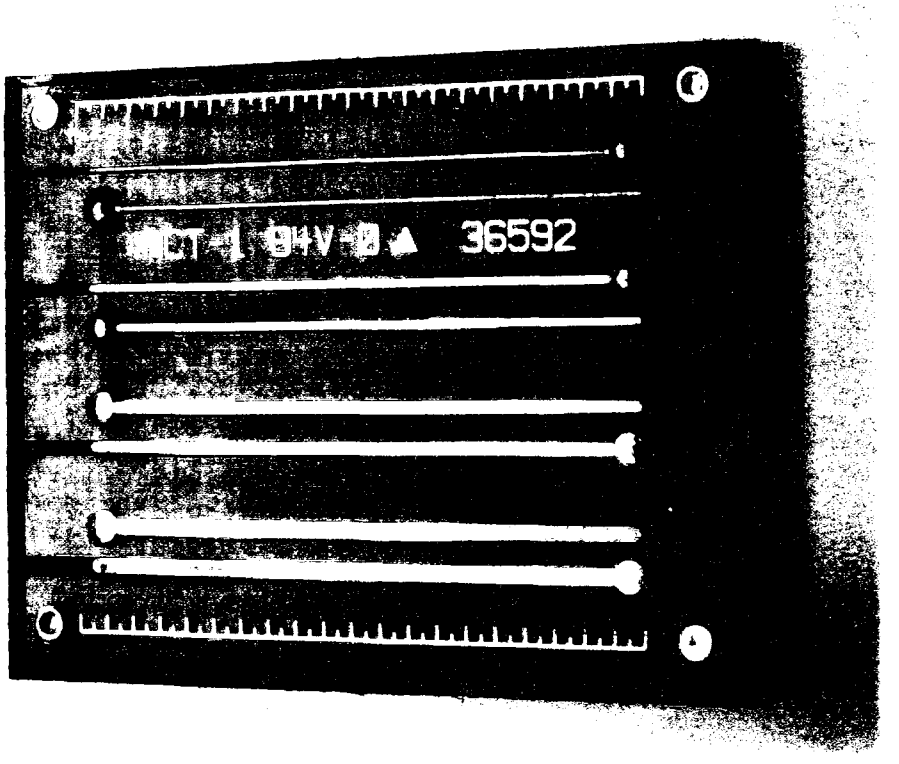

Figure 4. The capillary flow test vehicle. Depending on the ratio δ/ρ solder flows onto the strip to a distance that provides capillary pressure equilibrium.

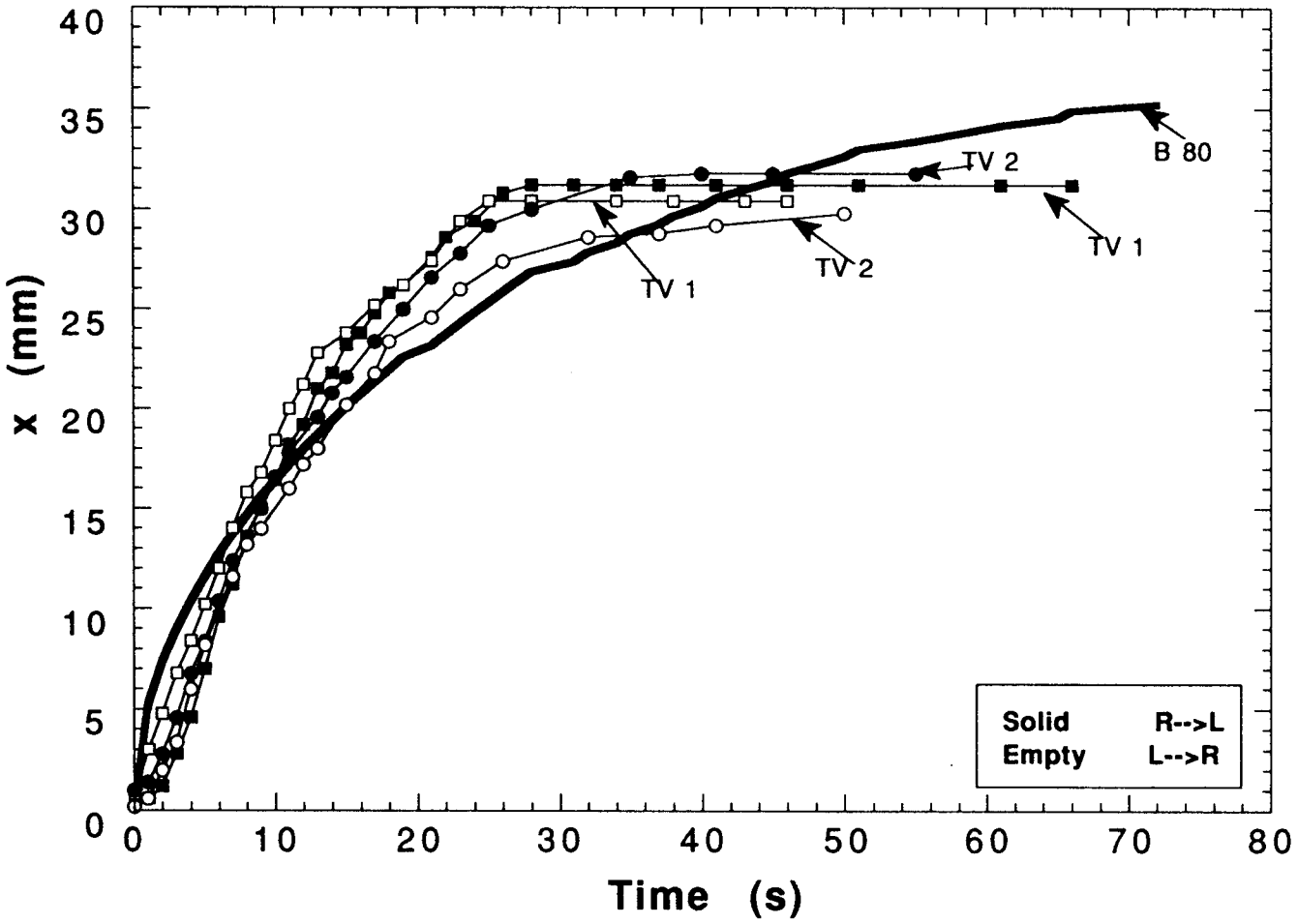

Figure 5a. Wetting results on test vehicles 1 and 2 distinguished according to number and flow direction. The average flow rate was 0.15 cm/s and a reasonable fit to the kinetics model gave B=80.

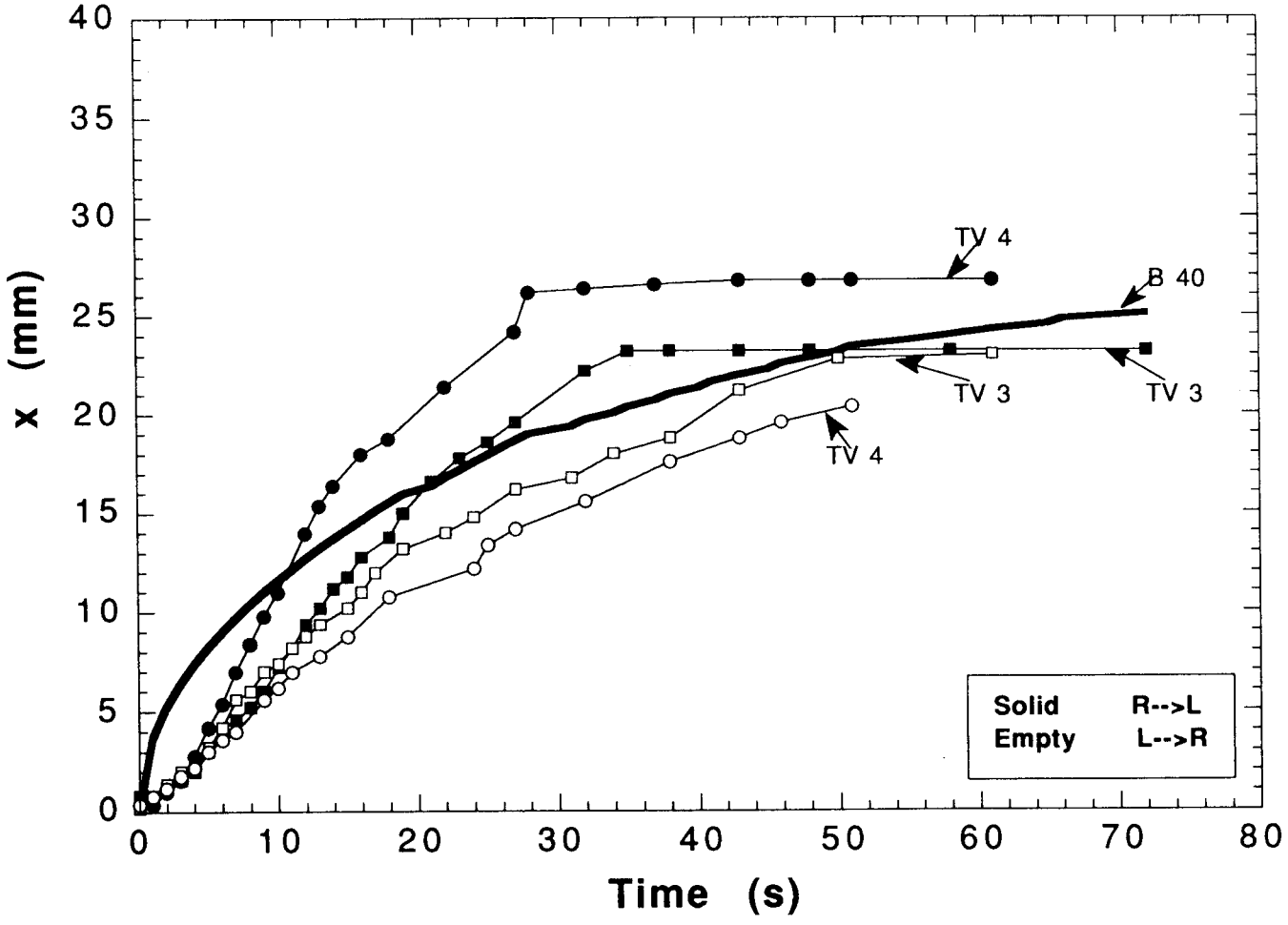

Figure 5b. Wetting results on test vehicles 3 and 4 distinguished according to number and flow direction. The average flow rate was 0.075 cm/s and a reasonable fit to the kinetics model gave B=40.

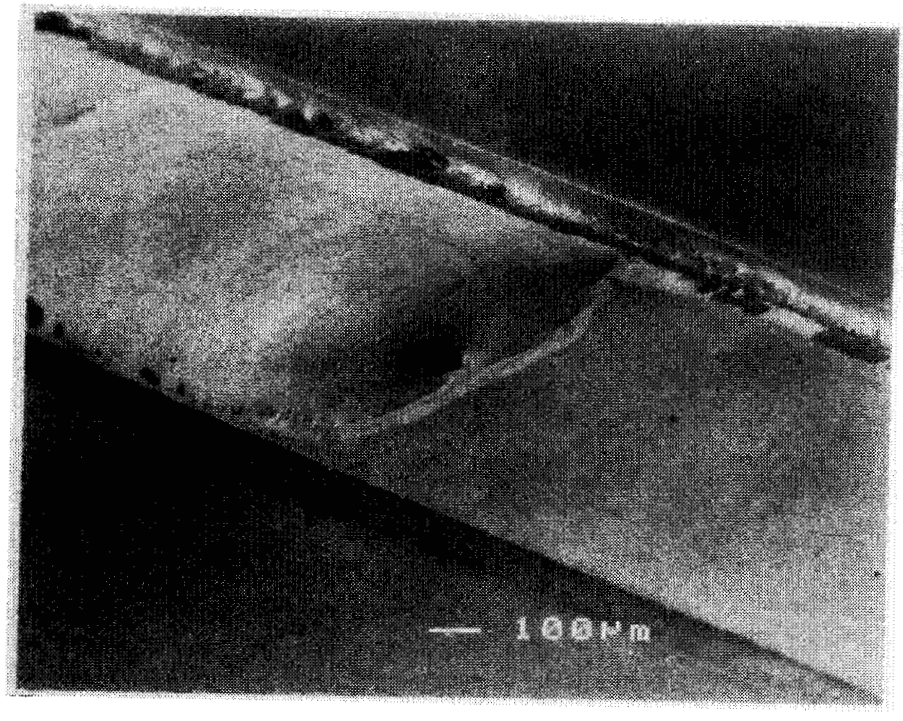

Figure 6. A scanning electron photomicrograph showing the wetting front. A reaction zone can be seen at the three phase line.

External Distribution:

1 Dr. J. Lee Parker
AT&T
4500 Laburnum Avenue
Richmond, VA 23231

1 Mr. George Wenger
AT&T-ERC
P.O. Box 900
Princeton, NJ 08540-0900

1 Dr. Bob Opila
AT&T
Bell Laboratories
600 Mountain Avenue
Murray Hill, NJ 07974

1 Dr. Ed Fey
IBM
1701 North Street
Bldg. 257-2
Endicott, NY 13760

1 Mr. Jim Reed
Texas Instruments
P.O. Box 149149
Austin, TX 78714-9149

1 Alan Burkett
Texas Instruments
2501 S. Highway 121
P.O. Box 4053464
Lewisville, TX 75067

1 Mr. Charles DeSantis
United Technologies Corporation
Hamilton Standard Division
One Hamilton Road
Windsor Locks, CT 06096-1010

1 Mr. Jay Kokas
United Technologies Corporation
Hamilton Standard Division
One Hamilton Road
Windsor Locks, CT 06096-1010

25 Mr. Ron Evans
NCMS
3025 Boardwalk
Ann Arbor, MI 48108-1779

1 Ms. Tracy Pattok
NCMS
3025 Boardwalk
Ann Arbor, MI 48108-1779

1 Dr. John R. Manning
NIST
Materials Bldg. A 153
Gaithersburg, MD 20899

Internal Distribution:

3	MS	0161	M. Moss, 11510
1		0957	G. L. Cessac, 2411
1		0336	A. K. Hays, 1709
1		0337	A. D. Romig, 1800
1		0340	J. L. Jellison, 1800A
1		0340	M. Essien, 1831
1		0340	C. L. Hernandez, 1831
1		0340	E. A. Holm, 1831
25		0340	F. M. Hosking, 1831
25		0340	D. O. MacCallum, 1831
1		0340	J. A. Rejent, 1831
1		0340	P. T. Vianco, 1831
25		0340	S. J. Sackinger, 1831
25		0340	F. G. Yost, 1831
1		0340	R. Salzbrenner, 1832
25		0340	D. R. Frear, 1832
1		0340	N. R. Sorensen, 1832
1		0340	M. J. Cieslak, 1831
1		0367	C. L. Renschler, 1812
1		0367	D. E. Peebles, 1812
1		0368	H. C. Peebles, 1815
1		9018	Central Tech. Files, 8523-2
5		0899	Technical Library, 7141
1		0619	Tech. Publications, 7151
2		0100	Document Processing for DOE/OSTI, 7613-2